Figure 7 Kimura et al

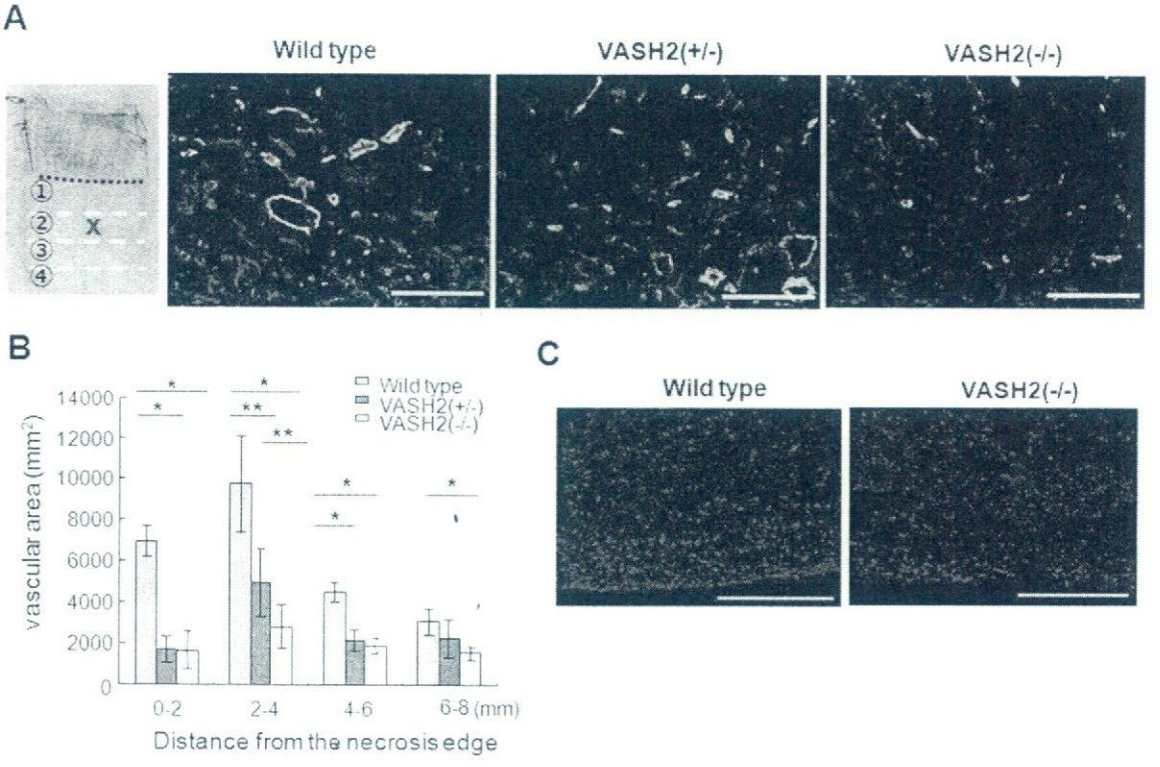

Figure 7 Kimura et al

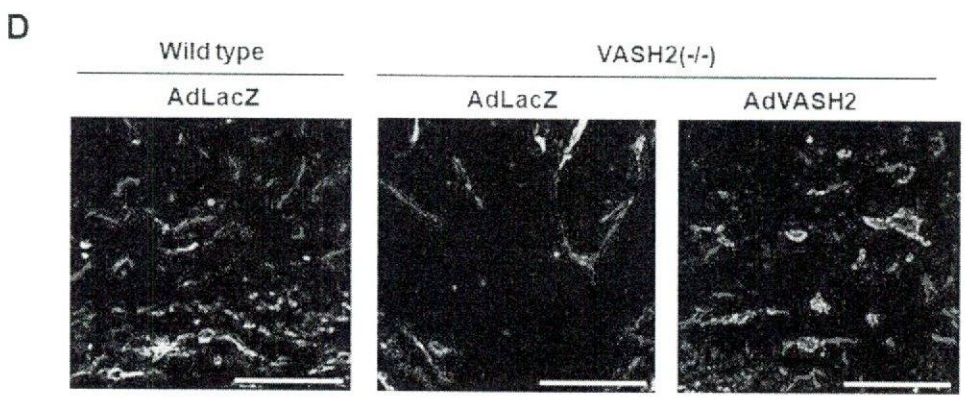

Diabetologia (2009) 52:359–361
DOI 10.1007/s00125-008-1229-z

RESEARCH LETTER

Vitreous levels of vasohibin-1 and vascular endothelial growth factor in patients with proliferative diabetic retinopathy

H. Sato · T. Abe · R. Wakusawa · N. Asai · H. Kunikata · H. Ohta · H. Sonoda · Y. Sato · K. Nishida

Received: 20 October 2008 / Accepted: 4 November 2008 / Published online: 5 December 2008

Keywords Angiogenesis · Proliferative diabetic retinopathy · Vascular endothelial growth factor · Vasohibin-1

Abbreviations
PDR proliferative diabetic retinopathy
PEDF pigment epithelium-derived factor
VEGF vascular endothelial growth factor

H. Sato (✉) · R. Wakusawa · H. Kunikata · K. Nishida
Department of Ophthalmology and Visual Science,
Tohoku University Graduate School of Medicine,
1-1 Seiryo-machi, Aoba-ku,
Sendai 980-8574, Japan
e-mail: hasato@oph.med.tohoku.ac.jp

T. Abe
Division of Clinical Cell Therapy,
Center for Translational and Advanced Animal Research,
Tohoku University Graduate School of Medicine,
Sendai, Japan

N. Asai
Department of Biochemistry and Biotechnology,
Division of Cell Technology,
Faculty of Agriculture and Life Science, Hirosaki University,
Hirosaki, Japan

H. Ohta · H. Sonoda
Shionogi Research Laboratories, Shionogi & Co. Ltd.,
Osaka, Japan

Y. Sato
Department of Vascular Biology, Institute of Development,
Aging, and Cancer, Tohoku University,
Sendai, Japan

To the Editor: Intraocular neovascularisation develops in many ischaemic retinal diseases, e.g. diabetic retinopathy, ischaemic retinal vein occlusion and retinopathy of prematurity. The new vessels are fragile and often rupture, leading to vitreous haemorrhage, tractional retinal detachment, neovascular glaucoma and subsequent vision decrease. The formation of new vessels is dependent on a local balance of stimulators and inhibitors of angiogenesis [1]. Among the stimulators, vascular endothelial growth factor (VEGF) has been shown to play a major role in mediating active neovascularisation in patients with diabetic retinopathy [2]. In addition, several studies have shown that the concentration of VEGF in the intraocular fluids was significantly elevated in eyes with proliferative diabetic retinopathy (PDR) [3–5]. On the other hand, pigment epithelium-derived factor (PEDF) is a potent inhibitor of angiogenesis, and lower levels of PEDF have been found in the vitreous of eyes with active diabetic retinopathy [4]. It has also been shown that the vitreous level of endostatin, another inhibitor of angiogenesis, is correlated with the level of VEGF and that endostatin is produced in the fibrovascular membrane of eyes with PDR [5].

Vasohibin-1, a novel angiogenesis inhibitor, is mainly produced in endothelial cells and is induced by stimulation with VEGF or fibroblast growth factor 2. Vasohibin-1 selectively affects endothelial cells and inhibits angiogenesis [6]. We therefore hypothesised that vasohibin-1 is present in the vitreous of eyes with PDR and is associated with the vitreous level of VEGF. To examine this hypothesis, we measured the vitreous levels of vasohibin-1 and VEGF in 49 samples from 46 patients. This study was conducted in accordance with the tenets of the Declaration of Helsinki as revised in 2000 and was carried out with the approval of the Institutional Review Board of Tohoku University. Informed consent was obtained from all patients

after an explanation of the purpose and procedures of the study.

The level of VEGF, measured by ELISA, was significantly higher in the vitreous samples from patients with PDR↑ (584.0±641.5 ↑pg/ml ↑[mean±SD]; n=37) than in samples from control patients with idiopathic macular hole or idiopathic epiretinal membrane (19.61±19.80 pg/ml; n=12; p=0.004; Student's t test). Western blot analysis using anti-vasohibin-1 mouse monoclonal antibody showed a 42 kDa band and/or a 36 kDa band of different intensity levels in 34 (92%) of the 37 vitreous samples of patients with PDR (Fig. 1a). No signal was detected in any control samples. To investigate the association between the vitreous levels of vasohibin-1 and VEGF, we determined the band intensity of the samples relative to that of given recombinant vasohibin-1 (100 fmol) using the publicly available ImageJ software (National Institutes of Health, Bethesda, MD, USA; http://rsb.info.nih.gov/ij/). We observed a statistically significant correlation between the vitreous concentration of vasohibin-1 and VEGF in the 37 samples with PDR (r=0.469, p=0.005; Spearman correlation coefficient by rank test) (Fig. 1b).

What is the source of the 42 kDa and 36 kDa forms of vasohibin-1 seen in the vitreous samples and detected by western blotting? An earlier study reported that the 36 kDa form was generated by processing the 42 kDa form and that both forms had anti-angiogenesis activity [7]. The forced production of vasohibin-1 in HUV-SV8 cells demonstrated that secreted vasohibin-1 is mostly the larger 42 kDa form and that the other major form (36 kDa) of the protein accumulates within the cells or pericellular milieu [7]. In our study, immunohistochemical analysis showed that vasohibin-1 was produced in the fibrovascular membranes of eyes with PDR (Fig. 1c,d). We suggest that one of the sources of vasohibin-1 is the endothelial cells in the fibrovascular membranes. As the blood–retina barrier in eyes with PDR is damaged, we cannot completely exclude the possibility that the vasohibin-1 in the vitreous cavity was from the blood. However, the concentration of vasohibin-1 in the plasma for the samples available from patients with PDR was very low (1.8±2.6 fmol/ml [mean±SD]; n=7) and was not statistically correlated with that in the vitreous (r=0.259, p=0.54; Spearman correlation coefficient by rank test), suggesting that the vasohibin-1 in the vitreous is mostly derived from the intraocular tissues. It remains to be determined whether the production of vasohibin-1 in the retinas of eyes with PDR is upregulated and whether vasohibin-1 is secreted into the vitreous cavity, because vasohibin-1 is produced in retinal cells as well as endothelial cells in normal mouse retinas [8].

Hypoxia induces VEGF, VEGF induces the production of vasohibin-1 in endothelial cells and vasohibin-1 inhibits angiogenesis as a negative feedback regulator [6]. On the other hand, hypoxia, as well as inflammatory cytokines (e.g. TNF-α and IL-1β, levels of which are increased in the vitreous of eyes with PDR), may reduce the VEGF-stimulated induction of vasohibin-1 in endothelial cells [6]. Many growth factors play an important role in the complex pathogenesis of diabetic retinopathy, in which hypoxia triggers angiogenesis. The results of this study show that the vitreous level of vasohibin-1 was positively correlated with that of VEGF, which suggests that vaso-

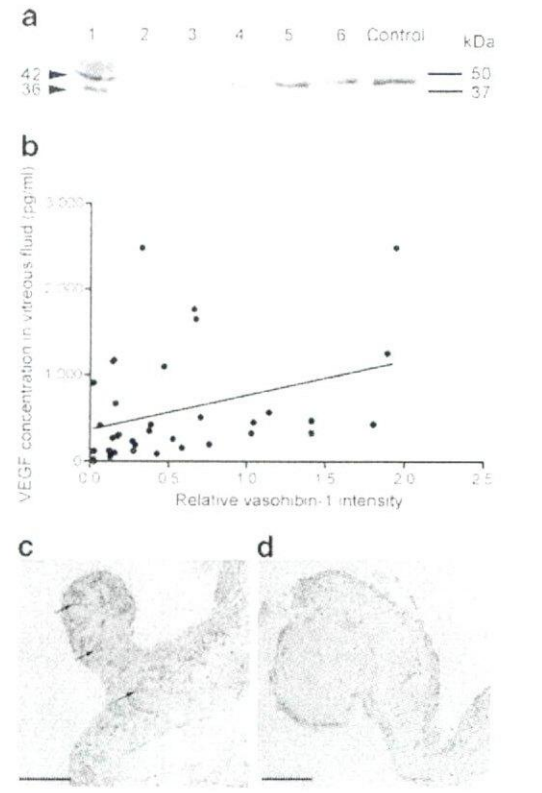

Fig. 1 **a** Detection of vasohibin-1 in vitreous fluid. Western blot shows 42 kDa and/or 36 kDa vasohibin-1 bands in each 7.5 μl of undiluted vitreous samples. Six vitreous samples (lanes 1–6) and 100 fmol recombinant vasohibin-1 (control) were loaded in this representative western blot. **b** Correlation between the vitreous concentration of vasohibin-1 and VEGF (r=0.469, p=0.005; Spearman correlation coefficient by rank test). The band intensities in the western blots were determined by ImageJ software. Relative vasohibin-1 intensity was calculated as the ratio of sample band intensity to control band intensity. Sample band intensity represents the sum of the 42 and 36 kDa vasohibin-1 bands. Exposure time of western blot was fixed to 30 s before the bands were saturated. Western blot analyses were performed in duplicate for each sample. VEGF concentration in the vitreous fluid was measured by ELISA using a human VEGF immunoassay (R&D Systems, Minneapolis, MN, USA). **c** Expression of vasohibin-1 in the surgically removed fibrovascular membranes of eyes with PDR. Fibrovascular membrane contains many new vessels. Immunohistochemistry using anti-vasohibin-1 mouse monoclonal antibody showed signals in the endothelial cells (arrows). **d** Absorbed antibody was used for the controls; no significant signal was seen. Scale bars, 100 μm

hibin-1 regulates retinal angiogenesis as an inhibitor. An intraocular injection of recombinant vasohibin-1 strongly suppressed retinal neovascularisation in mice with ischaemic retinopathy [9], suggesting that vasohibin-1 could be a good candidate for development as a therapeutic agent for diabetic retinopathy, especially in terms of mechanisms different from those in anti-VEGF therapy.

Acknowledgements We gratefully acknowledge the technical assistance of H. Seto.

Duality of interest The authors declare that there is no duality of interest associated with this manuscript.

References

1. Folkman J (1995) Angiogenesis in cancer, vascular, rheumatoid and other disease. Nat Med 1:27–31
2. Miller JW, Adamis AP, Aiello LP (1997) Vascular endothelial growth factor in ocular neovascularization and proliferative diabetic retinopathy. Diabetes Metab Rev 13:37–50
3. Aiello LP, Avery RL, Arrigg PG et al (1994) Vascular endothelial growth factor in ocular fluid of patients with diabetic retinopathy and other retinal disorders. N Engl J Med 331:1480–1487
4. Ogata N, Nishikawa M, Nishimura T, Mitsuma Y, Matsumura M (2002) Unbalanced vitreous levels of pigment epithelium-derived factor and vascular endothelial growth factor in diabetic retinopathy. Am J Ophthalmol 134:348–353
5. Funatsu H, Yamashita H, Noma H et al (2003) Outcome of vitreous surgery and the balance between vascular endothelial growth factor and endostatin. Invest Ophthalmol Vis Sci 44:1042–1047
6. Watanabe K, Hasegawa Y, Yamashita H et al (2004) Vasohibin as an endothelium-derived negative feedback regulator of angiogenesis. J Clin Invest 114:898–907
7. Sonoda H, Ohta H, Watanabe K, Yamashita H, Kimura H, Sato Y (2006) Multiple processing forms and their biological activities of a novel angiogenesis inhibitor vasohibin. Biochem Biophys Res Commun 342:640–646
8. Wakusawa R, Abe T, Sato H et al (2008) Expression of vasohibin, an antiangiogenic factor, in human choroidal neovascular membranes. Am J Ophthalmol 146:235–243
9. Shen J, Yang X, Xiao WH, Hackett SF, Sato Y, Campochiaro PA (2006) Vasohibin is up-regulated by VEGF in the retina and suppresses VEGF receptor 2 and retinal neovascularization. FASEB J 20:723–725

Cancer Gene Therapy (2008), 1–12

www.nature.com/cgt

ORIGINAL ARTICLE

Transcriptional silencing of ETS-1 efficiently suppresses angiogenesis of pancreatic cancer

LP Lefter[1,2], S Dima[3], M Sunamura[2], T Furukawa[4], Y Sato[5], M Abe[5], M Chivu[6], I Popescu[3] and A Horii[4]

[1]Department of Surgery, University of Medicine, Iasi, Romania; [2]Department of Gastroenterological Surgery, Tohoku University School of Medicine, Sendai, Japan; [3]Centre of Surgery and Liver Transplantation, Bucharest, Romania; [4]Department of Molecular Pathology, Tohoku University School of Medicine, Sendai, Japan; [5]Department of Ageing, Tohoku University School of Medicine, Sendai, Japan and [6]Stefan S Nicolau Institute of Virology, Bucharest, Romania

In this study, we addressed the hypothesis that transcriptional suppression of erythroblastosis virus E26 oncogene homolog 1 (ETS-1) is an efficient therapeutic approach to pancreatic adenocarcinoma by investigating the effect of ETS-1 suppression in human pancreatic cancer cells. We accomplished this by using an adenoviral vector encoding only the DNA-binding domain of wild-type ETS-1 (ETS-1 dominant negative, ETS-1-DN). ETS-1-DN decreases ETS-1-binding by competing for its binding to DNA. Adenoviral-mediated transfer of ETS-1-DN (adenoviral ETS-1-DN construct, AdETS-1-DN) into pancreatic tumor cell lines did not affect their proliferation rate *in vitro* but did significantly inhibit their *in vivo* growth in nude mice. Furthermore, to test the efficacy of ETS-1-DN *in vivo*, we injected the AdETS-1-DN into established human pancreatic adenocarcinomas grown in nude mice. This treatment significantly reduced tumor size as compared to saline injection, without any detectable side effects. Microvessel density in mouse xenografts displayed significantly lower values in tumors in which ETS-1 was downregulated. In addition, expression of the ETS-1-DN in the pancreatic cancer cells resulted in downregulation of urokinase-type plasminogen activator (u-PA) and metalloproteinase-1 (MMP-1) expression. Taken together, these data suggest that transcriptional inactivation of ETS-1 is able to significantly affect angiogenesis and growth of pancreatic cancer. This effect may be due in part to downregulation of MMP-1 and u-PA expression. Our results suggest that ETS-1-DN is a promising candidate for antiangiogenic gene therapy in pancreatic cancer. *Cancer Gene Therapy* advance online publication, 5 September 2008; doi:10.1038/cgt.2008.65

Keywords: ETS-1; angiogenesis; pancreatic cancer

Introduction

Although pancreatic ductal adenocarcinoma constitutes less than 2% of new cancer cases in the United States, it is the fifth leading cause of cancer-related deaths.[1] Considered by many to be one of the deadliest cancers, it is among the most studied malignancies and associated with a mean worldwide survival rate below 5%.[1,2] Although significant progress has been achieved with standard therapeutic approaches such as surgery, chemotherapy, or radiation, these approaches do not significantly improve the overall survival rate.[3] New vessel formation (angiogenesis) is a critical step in cancer progression. Clinical data have demonstrated that anti-vascular endothelial growth factor (VEGF) therapy with bevacizumab (an anti-VEGF specific antibody) is efficacious when combined with chemotherapy in colorectal and lung cancer.[4,5] Therefore, antiangiogenesis-based approaches aimed at preventing tumor vessel growth should be introduced to improve survival rates.[6]

However, a recent randomized phase 3 clinical study showed no benefit from bevacizumab in patients with pancreatic cancer. Thus, new antiangiogenic approaches are needed to treat this disease.

Controlled destruction of the principal barriers to tumor development and spread, that is, the basement membrane and extracellular matrix (ECM) compartments, is mostly influenced by the proteolytic activity surrounding a tumor mass. Although many factors regulate malignant tumor growth and spread, it is the protein profile within and interactions formed between a tumor and its microenvironment that are important for each step of tumor progression. The matrix metalloproteinases (MMPs) have recently been implicated in primary and metastatic tumor growth and angiogenesis;

Some data included in this article were presented at the 17th World Congress of the International Association of Surgeons, Gastroenterologists and Oncologists in Bucharest, Romania, on 5–8 September 2007.
Correspondence: Dr LP Lefter, Department of Surgery, St Spiridon University Hospital, 1 Independence Blv, Iasi 6600, Romania.
E-mail: lilefter@gmail.com
Received 3 March 2008; revised 3 June 2008; accepted 25 July 2008

they also be involved in tumor promotion.[7] The *MMP* genes are transcriptionally responsive to a wide variety of oncogenes, growth factors, cytokines and hormones.[8] Notably, several recent studies have highlighted the erythroblastosis virus E26 oncogene homolog 1 (ETS-1) protein, which interacts with the urokinase-type plasminogen activator (*u-PA*) gene enhancer and with the promoters of the stromelysin-1 and *MMP* genes. The proto-oncogene ETS-1 is the cellular progenitor of v-ETS, a viral oncogene found in the genome of the E26 acute leukemia retrovirus.[9,10]

ETS-1 is the original member of a growing family of transcription factors that now includes over 50 members, each characterized by a conserved DNA-binding domain (EBD). The EBD binds to a consensus DNA sequence centered on a core GGAA/T motif, which has been designated as the ETS-binding site.[11] The genes for several proteins, including u-PA, MMP-1, MMP-3, MMP-9, integrin β-3, and VE-cadherin, have been reported to be downstream targets of ETS-1 in endothelial cell.[12,13] In addition to their importance in normal cellular function,[14] ETS products have also been implicated in several malignant and genetic disorders, based on their particular target genes. It has been reported that ETS-1 activity is correlated with the tumorigenic progression of carcinoma cells of the stomach,[15] thyroid,[16] and pancreas.[17] These findings have focused our attention on the potential role of ETS-1 as a multifunctional target for antiangiogenic gene therapy. Several studies have used EBD to downregulate ETS-1 activity in capillary endothelial cells or glioma cells. ETS-1 positively regulates angiogenesis, and the elimination of ETS-1 activity by a dominant-negative molecule inhibits angiogenesis *in vivo*.[18,19] Using a similar assay, downregulation of ETS-1 interfered with the expression of integrin α5, which is known to accelerate invasive events such as migration and adhesion in glioma cells.[20]

Our hypothesis in undertaking this study was that transcriptional suppression of ETS-1 is an efficient therapeutic approach for pancreatic adenocarcinoma.

In the present study, we have examined the role of ETS-1 downregulation using a gene therapy approach in an animal model in which transductions were carried out either *ex vivo* or *in vivo*. We report here the data demonstrating the efficacy of this approach for blocking angiogenesis, and we concomitantly gained insights into the mechanisms involved. These results suggest that targeting ETS-1 may be a valid approach for treating pancreatic cancer.

Materials and methods

Cell lines

The pancreatic cancer cell lines used were: BxPC3, Panc-1 (American Type Culture Collection, Rockville, MD) and PCI-35 (kindly provided by Dr Hiroshi Ishikura at Hokkaido University). These lines were cultured according to the protocol provided by the suppliers. All cell lines are well characterized in terms of mutational status, as described in a previous report from our group.[21] A normal pancreatic ductal cell line HPDEC-6, a kind gift from Dr MS Tsao, University of Toronto, was propagated as originally described.[22] All cells were routinely monitored for *Mycoplasma* contamination as well as for mouse hepatitis, Sendai, and pneumonia viruses, and the results were consistently negative.

Adenoviral-mediated gene transfer experiments

Suppression of the ETS-1-binding activity was performed using an adenoviral vector encoding only the His-6-tagged EBD (ETS-1-binding domain) but lacking the transactivation domain and most of the automodulation module (adenoviral ETS-1-DN construct, AdETS-1-DN). The adenoviral constructs and transfection conditions have been described previously.[19,23] Briefly, adenovirus vector encoding dominant-negative Ets-1 was constructed by homologous recombination in 293 cells between the transfer cassette bearing the expression unit of dominant-negative Ets-1 and almost the entire adenovirus genome and restriction enzyme-digested adenovirus genome tagged with terminal protein.[19] The adenovirus was applied at a concentration of 1×108 plaque-forming units (PFU)/ml, and adenovirus with the genome carrying an enhanced green fluorescent protein (*GFP*) gene (Clontech, Palo Alto, CA) or lacZ were used as controls as described.[19] Infection efficiency was monitored by fluorescence, which showed expression in 80% of cells. Expression of recombinant protein was confirmed by western blot analysis. Conversely, to overexpress ETS-1, we used a similar vector (adenoviral ETS-1, AdETS-1) that encodes a full-length, His6-tagged ETS-1 protein.[19] Gene transfer in tumor cells was carried out using adenoviral vectors at varying multiplicity of infections (MOI) from 10 to 100 for 36 h. The *LacZ* gene transfer (AdLacZ) efficiency was assessed using β-galactosidase staining as described elsewhere.[24] We used the following nomenclature for the infected cells: BxPC3/ETS-1, BxPC3/ETS-1-DN, BxPC3/LacZ, PCI-35/ETS-1, PCI-35/ETS-1-DN, PCI-35/LacZ, Panc-1/ETS-1, Panc-1/ETS-1-DN, and Panc-1/LacZ. His6-tagged ETS-1 was detected by immunocytochemistry using an anti-His6 antibody (Sigma Chemical Co., St Louis, MO), according to the provider's protocol.

RT–PCR

Reverse transcription (RT)–PCR was performed using methods described previously.[25,26] Expression of the *hMSH2* gene was monitored as a positive control as the gene was demonstrated to be expressed in all parental cells.[27]

Samples of 29 primary human pancreatic cancers as well as the corresponding normal pancreatic tissues were also used. These tissues were obtained at Tohoku University Hospital with informed consent and were reviewed by a board-approved pathologist. The protocol was approved by the Ethical Board of Tohoku University Hospital.

Northern blotting

Extracted total RNA (10 μg) was subjected to electrophoresis on a 1% agarose gel containing 5% formalin and then transferred to a Hybond N+ membrane (Amersham, Sweden).[6] We also used human MTN blot membranes containing 16 tissues (Clontech). Probes for ETS-1 and β-actin were obtained from RT–PCR products. Direct sequencing using ABI Prism BigDye Terminator Cycle Sequencing Ready Reaction kit and a 310 DNA sequencer (Applied Biosystems, Foster City, CA) confirmed the sequences of these fragments. Digital autoradiography and quantification of the results were carried out using the BAS 1500 and Image Gauge 3.3 (Fujifilm, Japan) software.

Immunoblotting analysis

Western blotting was performed using 15–20 μg of total lysate as previously described.[28] Conditioned media were obtained, stored, and analyzed as previously described.[29] Primary antibodies used were: polyclonal rabbit anti-human ETS-1, goat anti-human MMP2 and MMP9 (Santa Cruz Laboratories, Santa Cruz, CA), monoclonal mouse anti-human β-actin (Sigma, St Louis, MO) anti-His6, and rabbit anti-human VEGF (Sigma). Secondary antibodies employed were: swine anti-rabbit, swine –anti-goat (Tago Inc., Burlingame, CA) and a sheep anti-mouse peroxidase-conjugated antibody (Amersham, Buckinghamshire, UK). A total lysate of HPDEC-6 was used as a positive control. Immunoreactivity was subsequently demonstrated using the enhanced chemiluminescence ECL western blotting kit (Amersham). The relative intensity of signals was analyzed using the Luminescent Image Analyzer LAS-1000 Plus and Image software Gauge 3.3 (FUJI Photo Film, Co. Ltd, Kanagawa, Japan).

DNA-binding activity, dual luciferase assay and electrophoretic mobility shift assay

DNA-binding assays for ETS-1 proteins were performed with 10 μg of nuclear extract, as described previously.[30] Competition assays were performed with a hundred-fold excess of unlabeled wild-type (WT) or mutant SBE (MT) oligonucleotides. For supershift assays, the nuclear extracts were incubated with 2 μl of ETS-1 antibodies for 30 min at room temperature before the addition of a labeled probe. Reactions were analyzed on a native 4% polyacrylamide gel and exposed to an imaging plate, which was then analyzed with a BAS 2000 image analyzer (Fuji, Tokyo, Japan).

Transfections and luciferase assays

Luciferase assays were conducted as described previously.[31] Briefly, the reporter construct was generated by inserting five head-to-tail ligated copies of the oligo 5′-TCGAGCAGGAAGTTTCG-3′, which contained the PEA3 ETS-binding site from the polyoma virus enhancer, into the pGL3-basic vector, which encoded firefly luciferase (FLS; Promega, Madison, WI). The cells were infected with AdETS-1, AdETS-1-DN or AdLacZ for 36 h at an MOI of 50. Each cell line was then seeded at 0.5×10^5 cells per 10-mm dish and incubated overnight at 37 °C in an incubator containing 5% CO_2. For each transfection, 0.1–0.3 μg of empty vector (pcDNA3; Invitrogen, Carlsbad, CA) and/or pRL-TK (Promega), along with 0.5–1 μg of promoter-luciferase DNA, were mixed together in 50 μl of Opti-MEM (Life Technologies Inc.), and a precipitate formed using LipofectAMINE 2000 (Life Technologies Inc.), according to the manufacturer's recommendations. The empty vector, pcDNA3, was used as a control for normalizing to total plasmid DNA. Cells were washed with Opti-MEM, and complexes were applied to the cells. After 36 h, *FLS* and renilla luciferase (*RLS*) gene activities in extracts from triplicate samples were sequentially measured by using a Dual Luciferase Reporter Assay System (Promega), according to the manufacturer's protocol. Measurements were performed automatically in a Luminescencer (Lumat LB 9507, Berthold, Germany), and results were expressed as fold increase compared to control cells.

In vitro *proliferation assays*

Anchorage-dependent proliferation was monitored by an 3-(4,5-dimethylthiazol-2-yl)-2,5-diphenyltetrazolium bromide (MTT) assay for 5 days, and a daily proliferation index was calculated for each parental and corresponding hybrid cell line using previously described methods.[32,33] The conversion of MTT to formazan dye was spectrometrically measured for absorbance at 590 nm, using a multi-well plate ImmunoReader System. All experiments were performed in duplicate sets of eight and repeated at least twice. Anchorage-independent proliferation (colony formation assay) was assessed in triplicate by two independent experiments as previously described.[31] The viable colonies were photographed using a Zeiss microscope with × 5 objective. Both colony number and size were measured and averaged using three randomly chosen photographs from each plate, employing NIH 1.62 software. Data were pooled, averaged and then statistically analyzed.

In vivo *proliferation assays*

Tissue sections of 5 μm thickness were prepared from formalin-fixed paraffin-embedded specimens. Immunohistochemical reactions were performed using a mouse anti-proliferating cell nuclear antigen (anti-PCNA, clone PC10, Dako Corporation) and developed with a Zymed Immunomouse kit (San Francisco, CA), as described previously.[34]

Proliferating cells were quantified by counting the PNCA-positive cells as well as the total cells in 10 arbitrarily selected fields (× 40 magnification) in a double-blinded manner. The percentage of PCNA-positive cells per 10 fields was calculated according to the following formula: (number of PCNA-positive cells)/(total number of cells) × 100. Negative control slides were prepared by omitting the primary antibody.

Determination of apoptosis

Apoptotic cells were detected by Annexin V/EGFP staining using an ApoAlert Annexin V-EGFP kit

obtained from Clontech. Stained cells were quantified using a Becton Dickinson FACScan, and data were analyzed using CellQuest software (version 3.1, Becton Dickinson).

Invasion assays

Invasion through Matrigel-reconstituted basement membrane was induced by seeding 5000 cells into the upper compartment of the invasion chamber (Becton Dickinson Labware, Franklin Lakes, NJ) using serum-free medium and allowing the cells to invade for 18 h.[29] The invading cells were stained and photographed ($\times 100$ magnification). Cells were counted and averaged, and the data were expressed as the number of migrated cells per high-power field. All experiments were performed in triplicate.

In vivo gene therapy experiments

Eight-week-old, male, severe-combined immunodeficient nude mice (Clea Japan Inc., Tokyo, Japan) were maintained under pathogen-free conditions and used in accordance with NIH guidelines. For these experiments, an animal model was employed in which transductions were carried out either *ex vivo* or *in vivo*. In the *ex vivo* transduction model, gene transfer in PCI-35 and Panc-1 cells was achieved using adenoviral vectors encoding for the gene *ETS-1*, *ETS-1/DN*, or *LacZ* for 36 h at an MOI ranging from 50 to 100. Logarithmically growing cells trypsinized from subconfluent monolayers were suspended in medium containing 25% Matrigel Growth Factor Reduced (Becton Dickinson Labware) at a density of 1×10^7 cells per ml. For each inoculation, 3×10^6 cells in 0.3 ml of suspension were injected s.c. into the hind flanks of five nude mice.[33] Data from independent experiments were pooled for statistical analysis. At week 8, when the control tumors reached approximately 2000 mm^3, the mice were killed. For the *in vivo* transduction we used a preestablished xenograft model. Cells were implanted by s.c. injection of 3×10^6 cells in 300 µl of culture medium containing 10% matrigel into the dorsal surface of the 15 mice. Tumors were allowed to develop for 5–7 days until a volume of approximately 100 mm^3 was reached, and then the mice were divided into three experimental groups. Each mouse received intratumoral (i.t.) inoculation with excipient only (phosphate-buffered saline), Ad/LacZ or Ad/ETS-1-DN (10^{10} PFU in 50 µl excipient) using a 32-gauge needle. Every animal received five i.t. injections spaced at 5-day intervals. The tumor diameters were measured before each injection with the use of a caliper. Mice were weighted and observed biweekly for monitoring of detectable side effects. One week after treatment was completed, the mice were killed and the tumors were excised for tissue sections.

Immunohistochemical analysis

Tumor samples were fixed overnight in phospholysine-paraformaldehyde, embedded in optimal cutting temperature compound (Sakura Finetechnical Co., Ltd., Tokyo, Japan) and stored at −80 °C. Tumor samples fixed in 10% formalin and then embedded in paraffin were also used. Tumors grown in nude mice as well as 29 primary human pancreatic tumors were immunostained using rabbit anti-human ETS-1 antibody (Santa Cruz Biotechnology Inc., Santa Cruz, CA) as previously described.[17] The degree of ETS-1 expression in the human samples was assessed according to a previously reported method.[17,35] All sections were reviewed independently by pathologists blinded to all clinical and pathologic information (TF and MA). The expression was graded on a scale from 0 to 3. A grade of 0 represented no stain uptake by malignant cells. Neoplastic cells were considered positive when they revealed cytoplasmic or membrane staining of at least moderate intensity and were graded as follows: grade 1, 1–33% positive cells; grade 2, 34–66% positive cells and grade 3, >66% cells positive. Normal ductal structures admixed in some tumor samples did not stain and served as internal negative controls. ETS-1 expression was considered positive when at least one of the pancreatic tissue intensity in >5% of pancreatic cancer cells. Immunohistochemical staining with an anti-PECAM-1 antibody (clone MEC13.3; Pharmingen, San Diego, CA) was performed as previously described.[36] Microvessel density was estimated by counting five non-overlapping areas of tumor infiltration (1 mm^2 area) and the data are presented as means of relative microvessel structures area (in pixels) ± s.d. The immunostaining of gelatinases (MMP-1 and MMP-2) was performed as previously described,[37,38] using goat anti-mouse antibodies (Santa Cruz Biotechnology Inc.).

Statistical analysis

A two-tailed Student's *t*-test was computed by GraphPad Prism 3.0 software (GraphPad Software Inc., San Diego, CA) and used to determine the statistical significance of measured differences. Statistical significance was judged based on *P*-values <0.05.

Results

Expression of ETS-1 in human pancreatic cancer tissues and cell lines

The status of ETS-1 expression was defined using three pancreatic cancer cell lines (BxPC3, Panc-1 and PCI-35), a normal pancreatic ductal cell line (HPDEC-6) and 29 different pancreatic cancer specimens from our tissue library. Endogenous ETS-1 was expressed in all the pancreatic cancer cells, based on mRNA (Figures 1a–c) or protein analysis (Figure 1d). In addition, apparently higher ETS-1 levels were found in SMAD4-null cell lines (Figures 1a–c, lines 1–2), in accordance with our previous findings.[6] The ETS-1 protein levels in human tissue samples appeared to correlate with tumor histology as previously reported.[17] ETS-1 expression was barely detectable in normal pancreatic ductal tissue (Figure 1f). However, whole RNA pancreatic extract (Figure 1e) revealed a relatively abundant expression of ETS-1. This differential expression was confirmed *in vitro* using cultured pancreatic ductal cells (HPDEC-6, Figure 1a, line 4). Remarkably, ETS-1 expression appeared stronger in the islets as compared with either normal or pancreatic

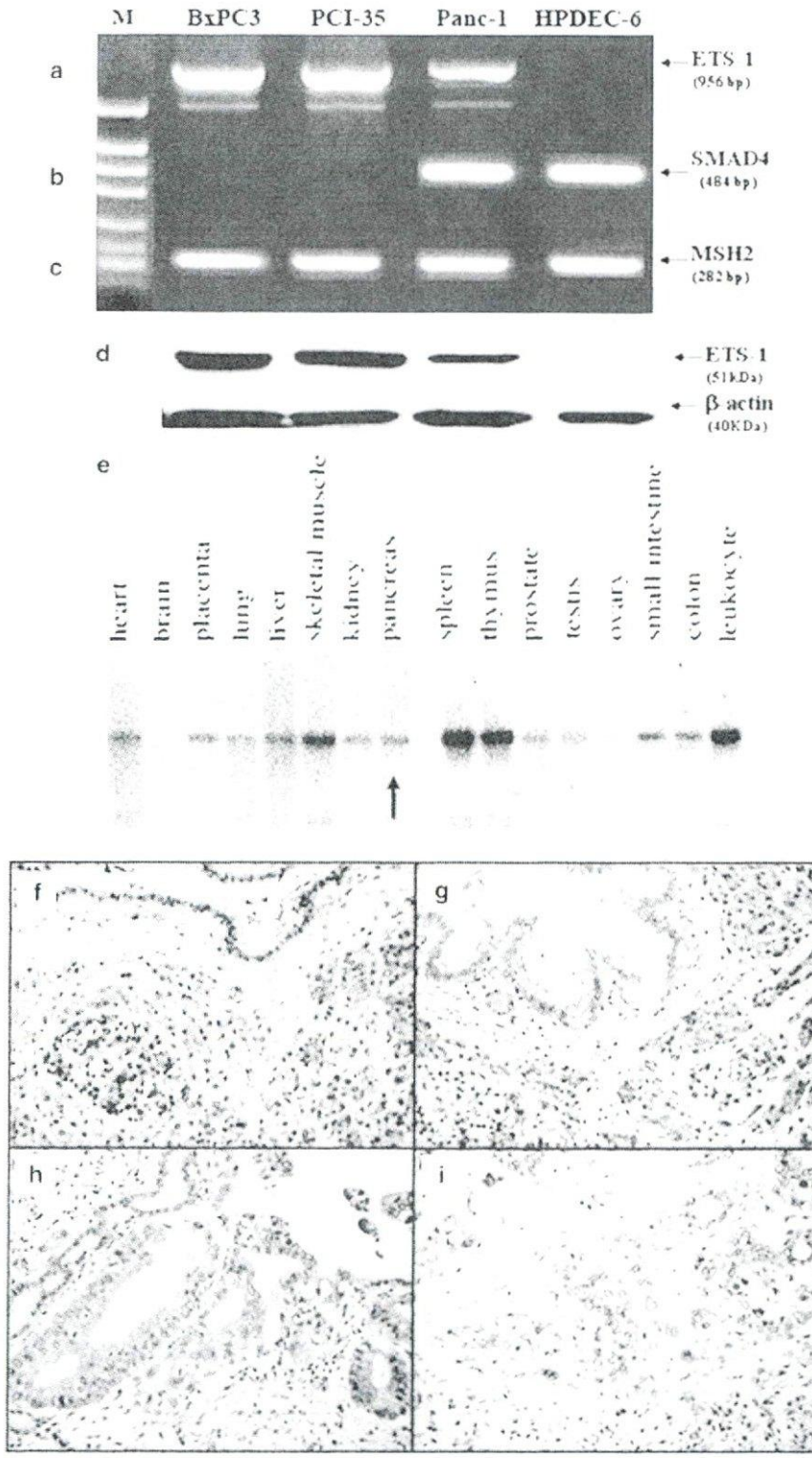

Figure 1 Expression of erythroblastosis virus E26 oncogene homolog 1 (ETS-1) in pancreatic cancer cells. Pancreatic cancer cells (**a**–**d**), normal pancreas (**e**, **f**), and different tissue types: dysplastic (**g**), moderate (**h**) and poorly (**i**) differentiated pancreatic cancers. PCR amplifications, immunostaining and western blotting were performed using anti-human ETS-1 antibodies as described in Materials and methods section. Original magnifications were × 400. Lane 1, BxPC3; lane 2, PCI 35; lane 3, Panc-1; lane 4, HPDEC-6. ETS-1 RNA expression in normal human tissues (**e**). The MTN RNA membranes containing 16 different normal tissues (Clontech) were probed with ^{32}P-labeled ETS-1 cDNA. Probes for ETS-1 and β-actin were obtained from reverse transcription (RT)–PCR products.

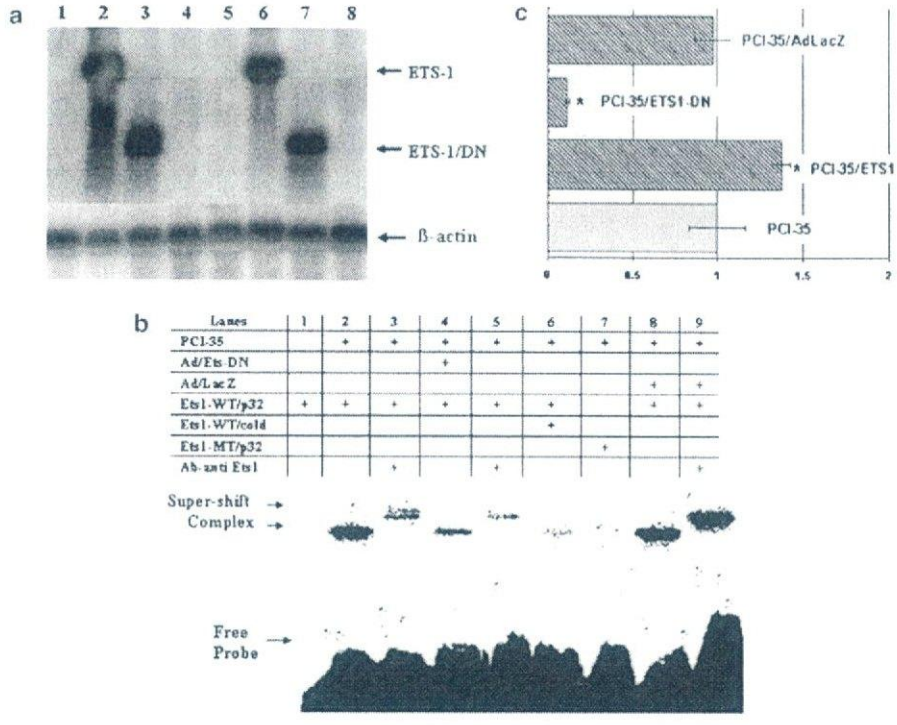

Figure 2 Pancreatic cancer expressing ETS-1 dominant negative (ETS-1-DN). Northern blotting analysis (**a**) was performed using 10 μg of total RNA, showing erythroblastosis virus E26 oncogene homolog 1 (ETS-1) or ETS-1-DN at the indicated levels. Lanes: 1, Panc-1; 2, Panc-1/ETS-1; 3, Panc-1/ETS-1-DN; 4, Panc-1/LacZ; 5, PCI-35; 6, PCI-35/ETS-1; 7, PCI-35/ETS-1-DN; and 8, PCI-35/LacZ. Electrophoretic mobility shift assays (**b**) were performed using an ETS-1-binding probe as described in Materials and methods section. Lanes: 1, unbound probe; 2 and 3, PCI-35/LacZ, 4 and 5, PCI-35/ETS-1-DN, 6 and 7, normal and mutant competitor, respectively. Transactivation of ETS-1 promoter activity (**c**) was accomplished by exogenously adding ETS-1 and ETS-1-DN. The indicated cells were infected with adenoviral ETS-1, adenoviral ETS-1-DN construct or AdLacZ for 36 h at an MOI of 50. Cells were subsequently transfected with pRL-TK (0.25 μg) and 1 μg of ETS-1 expression construct or control pcDNA3 vector, pcDNA3. Luciferase assays were performed after 36 h, and activity is reported as fold induction. Bars, ± s.d. in triplicate assays.

cancer tissues. Among the 29 cases of pancreatic adenocarcinoma, 24 (70.5%) showed positive staining for the ETS-1 protein. Of these, 18 had grade 2 expression and 6 had grade 3 expression. Overall, papillary carcinoma, well-differentiated adenocarcinoma (Figure 1g), and moderately differentiated adenocarcinoma (Figure 1h) expressed gradually higher levels of ETS-1. In contrast, poorly differentiated adenocarcinoma (six cases had grade 0 expression) expressed relatively low levels of ETS-1 (Figure 1i), suggesting that ETS-1 may play a more important role in the early stages of pancreatic tumorigenesis.

Pancreatic cancer cells expressing ETS-1-DN

Suppression of the ETS-1-binding activity was performed using an adenoviral vector encoding the His-6-tagged EBD but lacking the transactivation domain and most of automodulation module (AdETS-1-DN). The expression of exogenous ETS-1-DN RNA was first confirmed by northern blotting, demonstrating expression in transfected cells but not in noninfected or control virus-infected cells. Endogenous ETS-1 RNA was also detected in all parental and infected cells. The RNA levels of ETS-1-DN in PCI-35/ETS-1-DN and Panc-1/ETS-1-DN were significantly higher than those of endogenous ETS-1 (approximately 7- to 8-fold; Figure 2a). To examine the DNA-binding activity of the ectopically expressed ETS-1-DN protein, we performed electrophoretic mobility assays using a ^{32}P-labeled double-stranded ETS-1 probe, as previously described.[30] ETS-1-specific DNA-binding activities were detected to a similar extent in both WT and control cells (Figure 2b, lanes 2 and 8). Furthermore, ETS-1 specific DNA-binding activities appeared markedly reduced in the ETS-1-DN-infected cells (lane 4) when compared with those of parental or control infected cells (lanes 2 and 8). The cold competition experiments showed that the ETS-1/DNA-binding activity was specific (lanes 6), and supershift assays showed that the DNA-binding consisted of ETS-1 (lanes 3, 5 and 9). Moreover, a mutant ^{32}P-labeled ETS-1 probe failed to exhibit any binding activity (lane 7).

The ETS-1 transactivation activity was further analyzed using a luciferase construct containing an ETS-1-responsive promoter region. As shown in Figure 2c, ETS-1-DN significantly inhibited the transactivation activity of the construct. Taken together, these data show that suppression of functional activity of ETS-1 can be

Table 1 Oncogenic properties of the ETS-1-DN transfectants

Properties	*Cell lines*			
	PCI-35	*PCI-35/ETS-1-DN*	*PCI-35/ETS-1*	*PCI-35/AdLacZ*
(A) Anchorage-independent growth in soft agar, proliferation, invasion and apoptosis index. The averaged results ± s.d. from three independent experiments are represented[a]				
Proliferation index	9.3 ± 1.1	8.9 ± 0.95	9.6 ± 1.31	9.4 ± 1.21
Colony formation (number per 3-cm dish)	227 ± 19.13	231 ± 13.62	238 ± 18.61	225 ± 12.29
Colony size (μm)	384 ± 32.12	378.4 ± 16.21	381 ± 32.93	381 ± 29.66
Matrigel invasion assay[b]	1	0.38 ± 0.11	1.17 ± 0.14	0.97 ± 0.17
Apoptosis index (%)	2.81 ± 0.4	3.11 ± 0.5	2.97 ± 0.3	2.7 ± 0.2
(B) Tumorigenity and proliferating index of parental and hybrid cells in nude mice[c]				
Size of tumors (mm^3 at day 32)	1665 ± 245	356 ± 98	1716 ± 168	1732 ± 39
Latency period (days)	8 ± 2	14 ± 3	9 ± 3	8 ± 3
Microvessel area[d]	2231 ± 121	875 ± 87	2288 ± 106	2175 ± 112
Microvessel density	71 ± 9.6	22 ± 4.9	77 ± 11.6	79 ± 14.1
Proliferating index (PCNA positive cells per × 40 field)	17.7 ± 5.6	16.2 ± 5.1	16.7 ± 6.3	17.1 ± 4.4

Abbreviation: PCNA, proliferating cell nuclear antigen.
[a]The colony number and size were measured and averaged from three randomly chosen photographs of each plate, using NIH 1.62 software. Apoptotic cells were detected by Annexin V/EGFP staining. Data were quantified using a FACScan and analyzed using the CellQuest software.
[b]The invading cells were counted, averaged, and compared to the control cells.
[c]Representative averaged results ± s.d. from the triplicate experiments are shown. The latency period is defined as the period prior to tumors becoming palpable (about 5 mm in diameter).
[d]Microvessel area was quantified by HIH 1.62 software, and the data are presented as means of relative microvessel structures area (in pixels) ± s.d. Microvessel density was estimated by counting five non-overlapping areas of tumor infiltration (1 mm^2 area).

efficiently achieved by adenoviral-mediated gene transfer of a dominant-negative molecule.

ETS-1-DN reduces the vascular density and growth of pancreatic cancer xenografts but has no anti-tumor effect in vitro

Adenoviral-mediated transfer of ETS-1-DN (using AdETS-1-DN) in pancreatic tumor cell lines did not significantly affect their proliferation or degree of apoptosis *in vitro* (Table 1). Nevertheless, AdETS-1-DN-infected cells exhibited a significant decrease in their invasiveness through the matrigel-reconstituted basement membrane, as compared with parental control cells (Table 1). In contrast to the *in vitro* effect, ETS-1 downregulation significantly inhibited the *in vivo* tumor growth in nude mice injected with PCI-35 cells transduced with adenoviral vectors encoding ETS-1-DN, or LacZ (Figure 3a).

In an attempt to test the efficacy of ETS-1-DN as an *in vivo* gene therapy agent, we directly delivered the AdETS-1-DN into preestablished human pancreatic adenocarcinomas grown in nude mice. After the fifth injection, there was a nearly 70% reduction of tumor size in the AdETS-1-DN-treated group, as compared with the saline-injected control group ($P<0.05$), without detectable side effects (Figures 3b–d).

Microvessel density in mouse xenografts demonstrated significantly lower values in tumors with downregulated ETS-1 (Figures 4a and b). A 48% reduction ($P=0.026$) in microvessel density was seen in ETS-1-DN-treated tumors as compared with control cells. The expression of PCNA, a nuclear marker of cell proliferation, showed no significant difference between treated and control tumors (Table 1).

Transcriptional changes in pancreatic cancer cells upon ETS-1 blockade

The autocrine effect of ETS-1-DN in cancer cells was investigated by testing the changes in transcription of a panel of 10 known targets of ETS-1, such as VEGF, basic fibroblast growth factor (bFGF; data not shown), and proteases. Among these, expression of MMP-1 and u-PA were significantly downregulated by transcriptional suppression of ETS-1 (Figures 5a and b). This suggests that transcriptional inhibition of ETS-1 elicits antiangiogenic effects through dysregulation of proteolytic factor gene expression downstream of ETS-1 signaling.

Discussion

ETS transcription factors regulate many genes associated with tumor invasion, angiogenesis, cell adhesion, and organ development. The ETS family is comprised of more than 30 members that share a highly conserved DNA-binding motif termed the ETS domain.[39] In endothelial cells, the ETS-1-DNA-binding site has been reported to be included within the functional promoter site of many genes, including those encoding ECM-degrading enzymes like u-PA, MMP-1, MMP-3, MMP-9 and their inhibitors. Among them, the expression of several MMPs as well as u-PA was correlated with the progression of various cancers.[40,41]

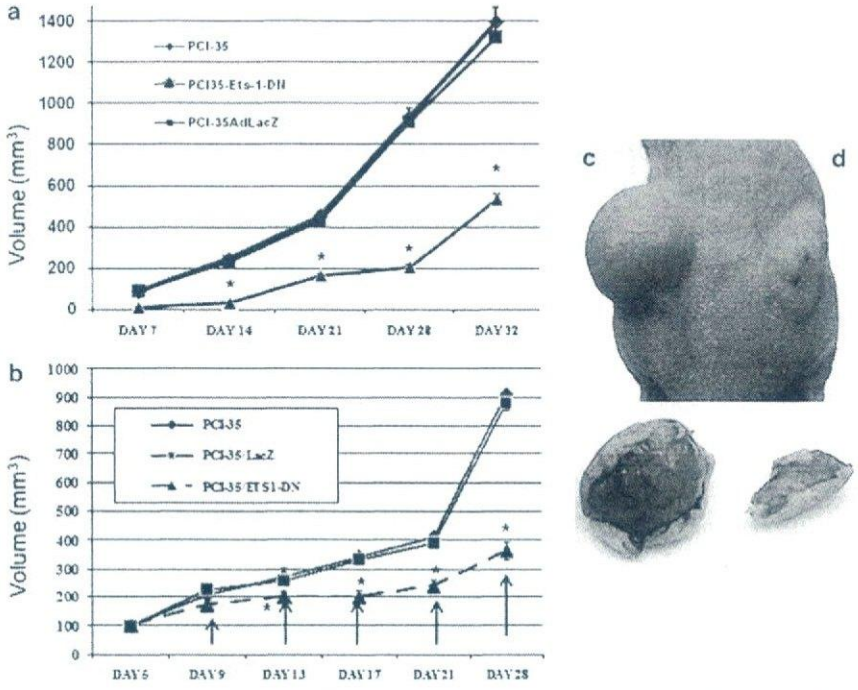

Figure 3 *In vivo* experiments. Logarithmically growing cells were suspended in medium containing 25% Matrigel. For each inoculation, 3×10^6 PCI-35 cells were transduced with adenoviral vectors encoding for erythroblastosis virus E26 oncogene homolog 1 (ETS-1), ETS-1 dominant negative (ETS-1/DN), or LacZ in a 0.3 ml suspension and injected s.c. into the hind flanks of nude mice. At week 8, when the control tumors reached approximately 2000 mm^3, the mice were killed (**a**). For the *in vivo* transduction therapy experiments, tumors were generated by s.c. injection of 3×10^6 cells in 300 μl of culture medium containing 10% Matrigel into the dorsal surface of mice (**b–d**). Tumors were allowed to develop for 5–7 days to about 100 mm^3 volume, and then mice were divided into three experimental groups. Each mouse received intratumoral (i.t.) inoculation with either excipient only (phosphate-buffered saline), Ad/LacZ, or Ad/ETS-1-DN (10^{10} PFU in 50 μl excipient). Each animal received five i.t. injections spaced at 5-day intervals. The tumor diameters were measured using a caliper before each administration. Data from independent experiments were pooled for statistical analysis.

Upregulation of ETS-1 expression has been documented in many types of human tumors. Generally, expression levels of ETS-1 correlate well with the grade of invasiveness and metastasis[42,43] and can therefore be useful for predicting the prognosis of cancer patients. It has been reported that expression of ETS-1 is correlated with the progression of carcinoma cells of the stomach,[15] thyroid,[16] and pancreas.[17] ETS-1 possesses a typical oncogene profile as judged by the correlation of its overexpression with the histological stages of many cancers, including glioma[20] and pancreatic cancer.[17] Although ETS-1 is strongly expressed in the moderately and well-differentiated pancreatic lesions, our data reveal that its levels were lower in poorly differentiated pancreatic cancers, suggesting that ETS-1 is inactivated by an unknown mechanism in these lesions. However, the latter quality was established by examining tumors derived from pancreatic cancer cell lines. Specifically, BxPC-3 produces moderately well-differentiated adenocarcinomas,[44] whereas Panc-1 maintains a poorly differentiated phenotype.[45] Furthermore, in an orthotopic pancreatic cancer model, marked differences with regard to tumor size, metastatic spread, and survival were found, depending on the grade of differentiation. Namely, less differentiated cells (Panc-1) caused higher dissemination scores and mortality than cells displaying greater differentiation. However, it is conceivable that the development of efficacious therapeutic treatments for human cancers relies significantly upon the presence and activity of the primary oncogene target.[46] In our study, the tumoral regression observed with local administration of Ad/ETS-1-DN appears to be significantly higher when the ETS-1 is abundantly expressed (Figure 1). However, IHC revealed that ETS-1 appears to be expressed more strongly in islets than in normal pancreatic ductal tissue or HPDEC-6 cells. To our knowledge, the significance, if any, of ETS-1 expression in the pancreatic islets is not known, and further focused studies may elucidate this phenomenon.

Expression of genes encoding for enzymes involved in degradation of the ECM, such as MMP-1, MMP-3, MMP-7 and MMP-9, is regulated by ETS family proteins such as ETS-1. Hence, it is highly suggestive that ETS-1 contributes to tumor invasion and progression through activation of these enzymes. Indeed, expression of these ECM remodeling enzymes is often detected along with c-ETS-1 mRNA in tumor cells, a phenomenon that correlates with poor survival in human ovarian carcinoma.[47] Moreover, ETS-1 is upregulated in human hepatocellular carcinoma (HCC), where it enhances expression of MMP-7, thus potentially contributing to the progres-

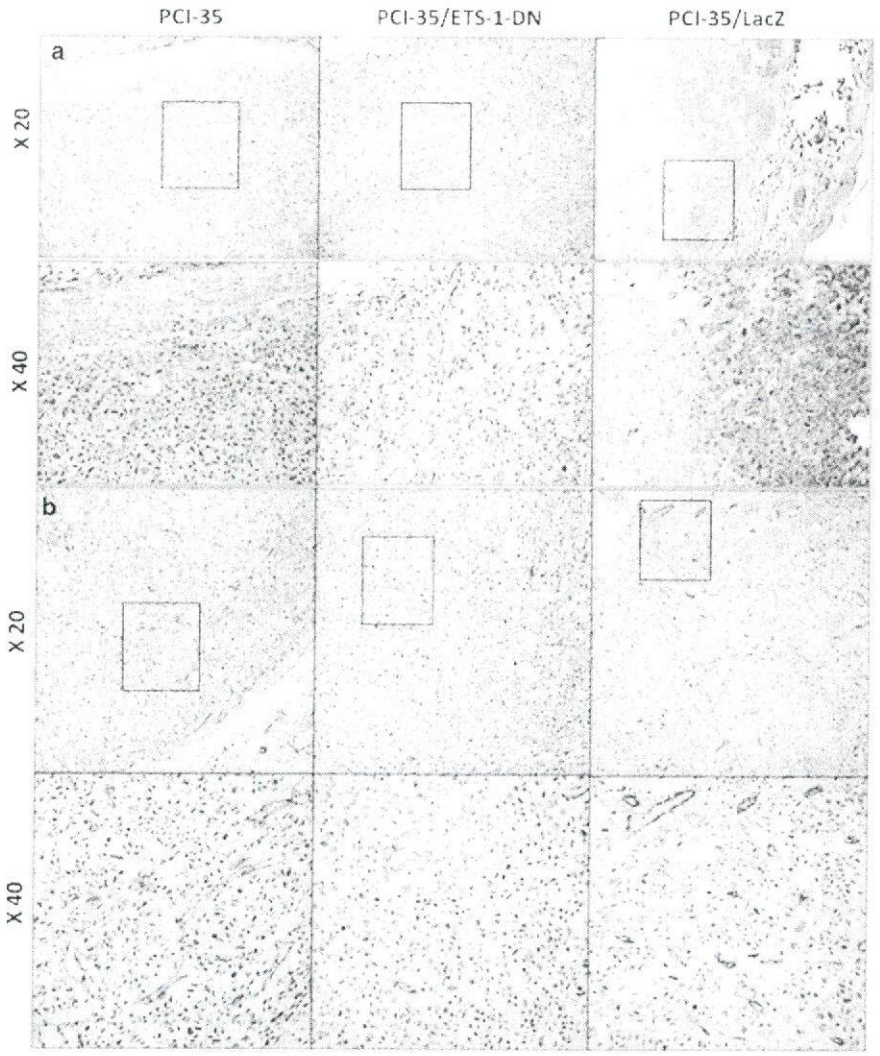

Figure 4 Representative data from immunohistochemical analysis of pancreatic cancer xenografts. Cells were infected as described in Materials and methods section and then inoculated s.c. in nude mice. At day 30, mice were killed and their tumors excised. Sections were stained with polyclonal rabbit anti-erythroblastosis virus E26 oncogene homolog 1 (ETS-1) antibody. A significant decrease of ETS-1 immunoreactivity was observed in ETS-1 dominant negative (ETS-1-DN) as compared with wild-type and ETS-1 tumors (**a**). Microvessel density was estimated using PECAM-1 reactivity. A 48% reduction in microvessel density was seen in ETS-1-DN-treated tumors as compared with control cells (**b**). Original magnifications are indicated on borders and the squares show the subsequently magnified area.

sion of HCC.[48] Although many potential target genes for the ETS family proteins have been identified, most studies have been carried out with the use of *in vitro* assays exclusively. Several studies used a truncated molecule containing EBD to downregulate ETS activity in capillary endothelial or glioma cells.[19,20] Hence, ETS-1 positively regulates angiogenesis, and using a dominant-negative molecule to eliminate ETS-1 activity resulted in angiogenesis inhibition *in vivo*. Consequently, we hypothesized that ETS-1 may be a useful target for gene therapy to combat the progression of pancreatic adenocarcinomas.

In this study, we have shown that ETS-1 is an effective target for gene therapy in pancreatic cancer using an animal model in which transductions were carried out either *ex vivo* or *in vivo*. We have investigated the effect of an ETS-1-DN molecule in a panel of three pancreatic cancer cells using *ex vivo* and *in vivo* gene therapy models. Adenoviral-mediated transfer of ETS-1-DN in pancreatic tumor cell lines did not affect their proliferation rate *in vitro*, but significantly delayed their *in vivo* growth in both nude mouse xenograft models used in this study. Our data clearly indicate that the ETS-1-DN molecule acted in a dominant-negative manner against ETS-1 by competing for its DNA-binding activity. In our system, the inhibition of the endogenous ETS-1 could not be completely abolished, results similar to those reported by Nakano *et al*.[19] using stable ETS-1-DN stable transfectants. This could be because of the use of transient transfections or to an autocrine loop that is able to restore ETS-1-binding activity. ETS-1 is also involved in angiogenesis, which is

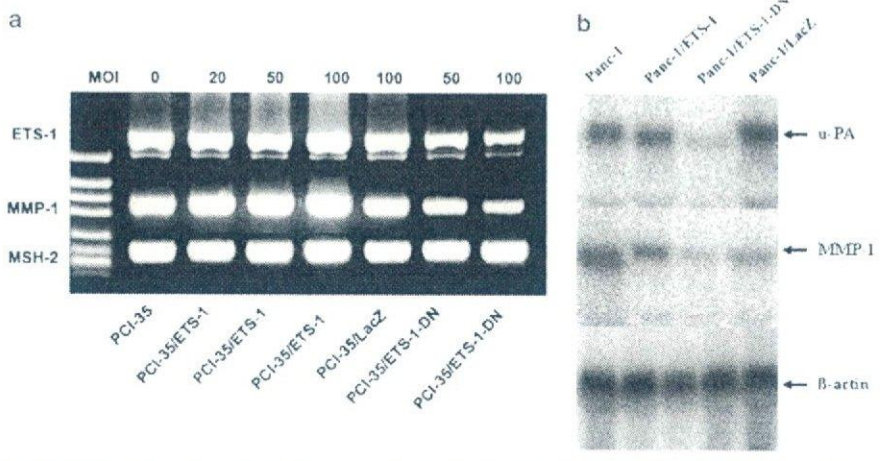

Figure 5 mRNA levels of metalloproteinase-1 (MMP-1) and urokinase-type plasminogen activator (u-PA). The mRNA levels of MMP-1 and u-PA were downregulated following adenoviral-mediated expression of the ETS-1 dominant negative (ETS-1-DN) molecule. PCI-35 and Panc-1 cells were infected with AdLacZ, AdETS-1, or AdETS-1-DN at the indicated MOI for 36 h. Reverse transcription (RT)–PCR showed a MOI-dependent downregulation of MMP-1 following ETS-1 transcriptional suppression (**a**). Panc-1 cells were infected with the above vectors at an MOI of 50 for 36 h, and then 10 μg of total RNA were subjected to northern blotting analysis (**b**). The blot was probed sequentially with u-PA, MMP-1 and β-actin probes.

essential for tumor progression. In fact, induction of ETS-1 expression appears to be a common phenomenon in endothelial cells following stimulation by angiogenic growth factors.[30] Angiogenesis is a necessary and required step for the transition from a small harmless cluster of cells to a large tumor, as well as for independent metastases.[49] We achieved a significant suppression of the tumor-induced angiogenesis by curtailing ETS-1-binding activity. It has been shown that VEGF and bFGF induce ETS-1 in endothelial cells, and ETS-1 then confers an angiogenic phenotype to endothelial cells through induction of u-PA and MMPs. In support of previous studies, our findings clearly indicate that the ETS-1-DN antiangiogenic effect is partly mediated through downregulation of MMP-1 and u-PA, both known downstream targets of ETS-1. Intriguingly, the expression levels of angiogenic factors such as VEGF, bFGF, MMP-2 and MMP-9, all well-known ETS-1 targets, were found to be unchanged by the experimental suppression of ETS-1 activity (data not shown). Nonetheless, such discrepancies appear to be based on differences in cellular make-up, which may include interactions between positive and negative regulators specific to different cell types.[50] For example, ETS-1 induces Fli-1 in endothelial cells but not in fibroblasts.[51]

Although demonstrating the efficiency of ETS-1-DN as an antiangiogenic agent, this study raises important questions regarding the deregulated targets downstream of ETS-1. Here, we demonstrated that downregulation of MMP-1 and u-PA occurs after transcriptional repression of ETS-1. It is conceivable that other known or unknown targets could be affected by the ETS-1 signaling cascade, and further mechanistic studies are warranted. However, the relevance of these future studies will depend upon the recognition of all the facets of the physiological roles of these transcription factors. Moreover, because the binding of ETS-1 to various ETS targets in certain tissues depends on the particular cellular context, future studies should identify the *in vivo* targets, including known or novel genes, in specific cell lineages. To this end, we are employing microarrays designed to reveal new targets downstream of ETS-1 signaling in pancreatic cancer.

Taken together, these results suggest that eliminating the ETS-1-binding activity efficiently suppresses the angiogenic and invasive abilities of pancreatic cancer cells. Moreover, this study indicates that ETS-1 should be considered a potential anticancer target for *in vivo* gene therapy in pancreatic cancer.

Abbreviations

AdETS-1-DN, adenoviral ETS-1-DN construct; EBD, ETS-1 DNA-binding domain; ETS-1, erythroblastosis virus E26 oncogene homolog 1; ETS-1-DN, ETS-1 dominant negative.

Acknowledgements

This work was supported by The Romanian National Authority for Scientific Research—CEEX 62 and 117 research grants—and the Japanese Ministries of Education, Culture, Sport, Science, and Technology.

References

1 Jemal A, Siegel R, Ward E, Murray T, Xu J, Thun MJ. Cancer statistics, 2007. *CA Cancer J Clin* 2007; **57**: 43–66.
2 Parker SL, Tong T, Bolden S, Wingo PA. Cancer statistics, 1997. *CA Cancer J Clin* 1997; **47**: 5–27.

3 Ariyama J, Suyama M, Ogawa K, Ikari T, Nagaiwa J, Fujii D *et al.* The detection and prognosis of small pancreatic carcinoma. *Int J Pancreatol* 1990; **7**: 37–47.
4 Sandler A, Gray R, Perry MC, Brahmer J, Schiller JH, Dowlati A *et al.* Paclitaxel-carboplatin alone or with bevacizumab for non-small-cell lung cancer. *N Engl J Med* 2006; **355**: 2542–2550.
5 Hurwitz H, Fehrenbacher L, Novotny W, Cartwright T, Hainsworth J, Heim W *et al.* Bevacizumab plus irinotecan, fluorouracil, and leucovorin for metastatic colorectal cancer. *N Engl J Med* 2004; **350**: 2335–2342.
6 Duda DG, Sunamura M, Lefter LP, Furukawa T, Yokoyama T, Yatsuoka T *et al.* Restoration of SMAD4 by gene therapy reverses the invasive phenotype in pancreatic adenocarcinoma cells. *Oncogene* 2003; **22**: 6857–6864.
7 Nelson AR, Fingleton B, Rothenberg ML, Matrisian LM. Matrix metalloproteinases: biologic activity and clinical implications. *J Clin Oncol* 2000; **18**: 1135–1149.
8 Kitamura T, Taketo MM. Keeping out the bad guys: gateway to cellular target therapy. *Cancer Res* 2007; **67**: 10099–10102.
9 Leprince D, Gegonne A, Coll J, de Taisne C, Schneeberger A, Lagrou C *et al.* A putative second cell-derived oncogene of the avian leukaemia retrovirus E26. *Nature* 1983; **306**: 395–397.
10 Nunn MF, Seeburg PH, Moscovici C, Duesberg PH. Tripartite structure of the avian erythroblastosis virus E26 transforming gene. *Nature* 1983; **306**: 391–395.
11 Ghysdael J, Boureux A. The ETS family of transcriptional regulators. In: Karin M (ed). *Oncogenes as Transcriptional Regulators*. Birkhauser: Basel, 1997.
12 Oda N, Abe M, Sato Y. ETS-1 converts endothelial cells to the angiogenic phenotype by inducing the expression of matrix metalloproteinases and integrin beta3. *J Cell Physiol* 1999; **178**: 121–132.
13 Lelievre E, Mattot V, Huber P, Vandenbunder B, Soncin F. ETS1 lowers capillary endothelial cell density at confluence and induces the expression of VE-cadherin. *Oncogene* 2000; **19**: 2438–2446.
14 Sementchenko VI, Watson DK. Ets target genes: past, present and future. *Oncogene* 2000; **19**: 6533–6548.
15 Nakayama T, Ito M, Ohtsuru A, Naito S, Nakashima M, Fagin JA *et al.* Expression of the Ets-1 proto-oncogene in human gastric carcinoma: correlation with tumor invasion. *Am J Pathol* 1996; **149**: 1931–1939.
16 Nakayama T, Ito M, Ohtsuru A, Naito S, Nakashima M, Sekine I. Expression of the ets-1 proto-oncogene in human thyroid tumor. *Mod Pathol* 1999; **12**: 61–68.
17 Ito T, Nakayama T, Ito M, Naito S, Kanematsu T, Sekine I. Expression of the ets-1 proto-oncogene in human pancreatic carcinoma. *Mod Pathol* 1998; **11**: 209–215.
18 Mattot V, Vercamer C, Soncin F, Calmels T, Huguet C, Fafeur V *et al.* Constitutive expression of the DNA-binding domain of Ets1 increases endothelial cell adhesion and stimulates their organization into capillary-like structures. *Oncogene* 2000; **19**: 762–772.
19 Nakano T, Abe M, Tanaka K, Shineha R, Satomi S, Sato Y. Angiogenesis inhibition by transdominant mutant Ets-1. *J Cell Physiol* 2000; **184**: 255–262.
20 Kita D, Takino T, Nakada M, Takahashi T, Yamashita J, Sato H. Expression of dominant-negative form of Ets-1 suppresses fibronectin-stimulated cell adhesion and migration through down-regulation of integrin alpha5 expression in U251 glioma cell line. *Cancer Res* 2001; **61**: 7985–7991.
21 Sun C, Yamato T, Furukawa T, Ohnishi Y, Kijima H, Horii A. Characterization of the mutations of the *K-ras*, *p53*, *p16*, and *SMAD4* genes in 15 human pancreatic cancer cell lines. *Oncol Rep* 2001; **8**: 89–92.
22 Furukawa T, Duguid WP, Rosenberg L, Viallet J, Galloway DA, Tsao MS. Long-term culture and immortalization of epithelial cells from normal adult human pancreatic ducts transfected by the *E6E7* gene of human papilloma virus 16. *Am J Pathol* 1996; **148**: 1763–1770.
23 Fujii M, Takeda K, Imamura T, Aoki H, Sampath TK, Enomoto S *et al.* Roles of bone morphogenetic protein type I receptors and Smad proteins in osteoblast and chondroblast differentiation. *Mol Biol Cell* 1999; **10**: 3801–3813.
24 Jiao S, Cheng L, Wolff JA, Yang NS. Particle bombardment-mediated gene transfer and expression in rat brain tissues. *Biotechnology (N Y)* 1993; **11**: 497–502.
25 Mori Y, Shiwaku H, Fukushige S, Wakatsuki S, Sato M, Nukiwa T *et al.* Alternative splicing of *hMSH2* in normal human tissues. *Hum Genet* 1997; **99**: 590–595.
26 Sunamura M, Lefter LP, Duda DG, Morita R, Inoue H, Yokoyama T *et al.* The role of chromosome 18 abnormalities in the progression of pancreatic adenocarcinoma. *Pancreas* 2004; **28**: 311–316.
27 Kondo E, Furukawa T, Yoshinaga K, Kijima H, Semba S, Yatsuoka T *et al.* Not *hMSH2* but *hMLH1* is frequently silenced by hypermethylation in endometrial cancer but rarely silenced in pancreatic cancer with microsatellite instability. *Int J Oncol* 2000; **17**: 535–541.
28 Kondo E, Horii A, Fukushige S. The human PMS2L proteins do not interact with hMLH1, a major DNA mismatch repair protein. *J Biochem* 1999; **125**: 818–825.
29 Attiga FA, Fernandez PM, Weeraratna AT, Manyak MJ, Patierno SR. Inhibitors of prostaglandin synthesis inhibit human prostate tumor cell invasiveness and reduce the release of matrix metalloproteinases. *Cancer Res* 2000; **60**: 4629–4637.
30 Iwasaka C, Tanaka K, Abe M, Sato Y. Ets-1 regulates angiogenesis by inducing the expression of urokinase-type plasminogen activator and matrix metalloproteinase-1 and the migration of vascular endothelial cells. *J Cell Physiol* 1996; **169**: 522–531.
31 Teruyama K, Abe M, Nakano T, Iwasaka-Yagi C, Takahashi S, Yamada S *et al.* Role of transcription factor Ets-1 in the apoptosis of human vascular endothelial cells. *J Cell Physiol* 2001; **188**: 243–252.
32 van Golen KL, Wu ZF, Qiao XT, Bao LW, Merajver SD. RhoC GTPase, a novel transforming oncogene for human mammary epithelial cells that partially recapitulates the inflammatory breast cancer phenotype. *Cancer Res* 2000; **60**: 5832–5838.
33 Lefter LP, Sunamura M, Furukawa T, Takeda K, Kotobuki N, Oshimura M *et al.* Inserting chromosome 18 into pancreatic cancer cells switches them to a dormant metastatic phenotype. *Clin Cancer Res* 2003; **9**: 5044–5052.
34 Zhu Z, Kleeff J, Kayed H, Wang L, Korc M, Buchler MW *et al.* Nerve growth factor and enhancement of proliferation, invasion, and tumorigenicity of pancreatic cancer cells. *Mol Carcinog* 2002; **35**: 138–147.
35 Khorana AA, Ahrendt SA, Ryan CK, Francis CW, Hruban RH, Hu YC *et al.* Tissue factor expression, angiogenesis, and thrombosis in pancreatic cancer. *Clin Cancer Res* 2007; **13**: 2870–2875.
36 Liao F, Li Y, O'Connor W, Zanetta L, Bassi R, Santiago A *et al.* Monoclonal antibody to vascular endothelial-cadherin

is a potent inhibitor of angiogenesis, tumor growth, and metastasis. *Cancer Res* 2000; **60**: 6805–6810.

37 Sun Y, Wenger L, Rutter JL, Brinckerhoff CE, Cheung HS. p53 down-regulates human matrix metalloproteinase-1 (Collagenase-1) gene expression. *J Biol Chem* 1999; **274**: 11535–11540.

38 Thant AA, Sein TT, Liu E, Machida K, Kikkawa F, Koike T *et al.* Ras pathway is required for the activation of MMP-2 secretion and for the invasion of src-transformed 3Y1. *Oncogene* 1999; **18**: 6555–6563.

39 Lelievre E, Lionneton F, Soncin F, Vandenbunder B. The Ets family contains transcriptional activators and repressors involved in angiogenesis. *Int J Biochem Cell Biol* 2001; **33**: 391–407.

40 Crawford HC, Scoggins CR, Washington MK, Matrisian LM, Leach SD. Matrix metalloproteinase-7 is expressed by pancreatic cancer precursors and regulates acinar-to-ductal metaplasia in exocrine pancreas. *J Clin Invest* 2002; **109**: 1437–1444.

41 Ellenrieder V, Hendler SF, Ruhland C, Boeck W, Adler G, Gress TM. TGF-beta-induced invasiveness of pancreatic cancer cells is mediated by matrix metalloproteinase-2 and the urokinase plasminogen activator system. *Int J Cancer* 2001; **93**: 204–211.

42 Behrens P, Rothe M, Wellmann A, Krischler J, Wernert N. The Ets-1 transcription factor is up-regulated together with MMP 1 and MMP 9 in the stroma of pre-invasive breast cancer. *J Pathol* 2001; **194**: 43–50.

43 Nakayama T, Ito M, Ohtsuru A, Naito S, Sekine I. Expression of the ets-1 proto-oncogene in human colorectal carcinoma. *Mod Pathol* 2001; **14**: 415–422.

44 Tan MH, Nowak NJ, Loor R, Ochi H, Sandberg AA, Lopez C *et al.* Characterization of a new primary human pancreatic tumor line. *Cancer Invest* 1986; **4**: 15–23.

45 Yunis AA, Arimura GK, Russin DJ. Human pancreatic carcinoma (MIA PaCa-2) in continuous culture: sensitivity to asparaginase. *Int J Cancer* 1977; **19**: 128–135.

46 Hotz HG, Reber HA, Hotz B, Yu T, Foitzik T, Buhr HJ *et al.* An orthotopic nude mouse model for evaluating pathophysiology and therapy of pancreatic cancer. *Pancreas* 2003; **26**: e89–e98.

47 Davidson B, Reich R, Goldberg I, Gotlieb WH, Kopolovic J, Berner A *et al.* Ets-1 messenger RNA expression is a novel marker of poor survival in ovarian carcinoma. *Clin Cancer Res* 2001; **7**: 551–557.

48 Ozaki I, Mizuta T, Zhao G, Yotsumoto H, Hara T, Kajihara S *et al.* Involvement of the *Ets-1* gene in overexpression of matrilysin in human hepatocellular carcinoma. *Cancer Res* 2000; **60**: 6519–6525.

49 Zetter BR. Angiogenesis and tumor metastasis. *Annu Rev Med* 1998; **49**: 407–424.

50 Oikawa T, Yamada T. Molecular biology of the Ets family of transcription factors. *Gene* 2003; **303**: 11–34.

51 Lelievre E, Lionneton F, Mattot V, Spruyt N, Soncin F. Ets-1 regulates fli-1 expression in endothelial cells. Identification of ETS binding sites in the *fli-1* gene promoter. *J Biol Chem* 2002; **277**: 25143–25151.

FEBS Letters 583 (2009) 308–312

FEBS Letters

journal homepage: www.FEBSLetters.org

A possible role of vimentin on the cell surface for the activation of latent transforming growth factor-β

Yasutake Nishida [a], Kenji Shibata [a], Motoo Yamasaki [a], Yasufumi Sato [b], Mayumi Abe [b,*]

[a] Innovative Drug Research Laboratories, Research Division, Kyowa Hakko Kirin Co. Ltd., Tokyo 194-8533, Japan
[b] Department of Vascular Biology, Institute of Development, Aging and Cancer, Tohoku University, Sendai 980-8575, Japan

ARTICLE INFO

Article history:
Received 24 November 2008
Revised 19 December 2008
Accepted 22 December 2008
Available online 31 December 2008

Edited by Masayuki Miyasaka

Keywords:
Latent TGF-β activation
Vimentin
LAP fragment
Avidin–biotin affinity
Proteolysis

ABSTRACT

Latent TGF-β (LTGF-β) has to be converted to active TGF-β for its activities. Previously, we reported that certain fragments of latency associated peptide (LAP) augmented LTGF-β activation via increase in binding of LTGF-β to the endothelial cell (EC) surface followed by cell-associated proteolysis. By searching for EC membrane proteins crosslinked with the LAP fragment, we identified the molecule bound to LAP fragment as vimentin. Moreover, the LAP fragment-induced LTGF-β activation was attenuated by anti-vimentin antibody. These results indicate that binding of the LAP fragment to vimentin on the cell surface is indispensable for LTGF-β activation by the LAP fragment.

Structured summary:
MINT-6806227: *vimentin* (uniprotkb:P48616) *binds* (MI:0407) to *LAP* (uniprotkb:P18341) by *competition binding* (MI:0405)
MINT-6806183: *LAP* (uniprotkb:P18341) *binds* (MI:0407) to *vimentin* (uniprotkb:P48616) by *cross-linking studies* (MI:0030).

1. Introduction

Transforming growth factor-β (TGF-β) is a multi-functional cytokine involved in a wide variety of process. TGF-β is synthesized and secreted as a latent complex composed of mature TGF-β, latency associated peptide (LAP) and latent TGF-β (LTGF-β) binding protein (LTBP) [1]. In order to execute its activities, TGF-β has to be converted from a latent form to an active one, namely mature TGF-β [1]. To date, various mechanisms for the activation of LTGF-β have been proposed including shear forces [2]. However, those can be mainly classified into two categories [1]. One is the structural change of LTGF-β through interaction with other molecules, such as thrombospondin-1 (TSP-1) [3] or integrin αvβ6 [4]. The other is the partial enzymatic cleavage or degradation of LTGF-β [5]. Among several enzymes that activate LTGF-β, the best-characterized one is plasmin, a serine protease, which removes LAP from LTGF-β [5,6]. We have focused on the activation mechanism involving in proteolysis on endothelial cell (EC) [6–9].

Targeting of LTGF-β to cell surface of ECs, where protease activities exist, is one of the important steps for LTGF-β activation. We developed a monoclonal antibody (mAb) against LAP (KM704). KM704 inhibited the activation of LTGF-β by blocking its binding to cells [7]. We assumed that the epitope of KM704 would be the binding site of LTGF-β to cell surface. Therefore, we synthesized several peptides containing the sequence of putative epitopes, and examined if the peptides inhibit the binding of LTGF-β. Surprisingly, some augmented its binding and enhanced LTGF-β activation, although none of them inhibited [9]. Next, we synthesized the relevant peptides supposed to be cleaved by plasmin from LAP, since plasmin activity on the cell surface seems to be necessary in the unique phenomenon [9]. One of the peptides, Peptide-25 (Leu132 to Arg152 in the LAP molecule) bound to EC surface, and increased binding of LTGF-β to there and the following LTGF-β activation [9].

The purpose of this study was to identify the cell surface binding molecule of Peptide-25. We identified the molecule bound to Peptide-25 as vimentin and confirmed that Peptide-25 specifically binds to vimentin protein on endothelial cell surface. Finally, we demonstrated that vimentin is involved in the LTGF-β activation.

* Corresponding author. Present address: Department of Nanomedicine (DNP), Tokyo Medical Dental University Graduate School, Tokyo 113-8549, Japan. Fax: +81 3 5803 4679.
E-mail address: mayudnp@tmd.ac.jp (M. Abe).

0014-5793/$34.00 © 2008 Federation of European Biochemical Societies. Published by Elsevier B.V. All rights reserved.
doi:10.1016/j.febslet.2008.12.051

To our knowledge, this is the first report to show that vimentin can play a role in TGF-β activation by the LAP fragment.

2. Materials and methods

2.1. Materials

Peptide-25, Peptide-25N, N-terminally biotin-labeled peptide and Peptide-21 were synthesized as previously described [9]. Bovine aortic endothelial cells (BAECs) were cultured in Dulbecco's modified eagle medium containing 10% fetal bovine serum (FBS) as previously described.

2.2. Cross-linking of Peptide-25N to the target molecule using BAECs

The confluent monolayers were crosslinked with 100 μM Peptide-25N using 2 mM Sulfo-EGS (Pierce Biotechnology, Rockford, IL) and harvested in detachment buffer (DB; 0.25 M sucrose, 0.3 mM PMSF, 10 mM Tris, 1 mM EDTA, pH 7.4, 10 μg/mL of leupeptin, antipain, and pepstatin, 50 μg/mL aprotinin, 100 μg/mL soybean trypsin inhibitor, 10 μg/mL bestatin and benzamidin hydrochloride, and 300 μM PMSF). In some experiments, cross-linking of Peptide-25N to the suspended cells was performed as described above and the precipitated cells were suspended in DB. Samples were stocked at −20 °C. The cells stocked were thawed, precipitated, and solubilized in reducing sample buffer for SDS–PAGE. To purify the target molecule, the membrane fraction was obtained in supernatant by solubilization in the buffer containing 8.5 M urea and 2% Nonidet P-40 and centrifugation.

2.3. Purification of a target molecule by avidin–biotin affinity chromatography and SDS–PAGE

The membrane fraction was applied onto the avidin–biotin affinity chromatography column (Ultralink Immobilized Monomeric Avidin Gel, Pierce Biotechnology) equilibrated with starting buffer (SB: 1.25 M urea, 2% NP-40, 125 mM NaCl, 10 mM Tris, 1 mM EDTA, pH 7.4). After washing the column with SB, strongly bound molecules including the target molecule of Peptide-25N were eluted in the buffer (2 M urea, 2% NP-40, 125 mM NaCl, 100 mM glycine, pH 2.8). The target molecules fractionated by the avidin–biotin affinity chromatography were precipitated by incubation in cold acetone at −20 °C over night, centrifuged, dried in vacuo, and applied to SDS–PAGE. The bands corresponding to the target complex containing Peptide-25N and to the co-eluted protein were cut out and extracted in reducing sample buffer at 37 °C over night. The purity of the target molecule preparation was confirmed by SDS–PAGE with Ag-staining using 2D-Silver Stain II "DAIICHI" (Daiichi Pure Chemicals, Tokyo, Japan).

2.4. Detection of the complex containing Peptide-25N by avidin staining

The proteins separated on SDS–PAGE were blotted onto a polyvinylidene fluoride (PVDF) membrane (Millipore, Billerica, MA) and the complex containing Peptide-25N was detected using avidin-biotinylated horseradish peroxidase (HRP) complex solution (Elite Vectastain ABC kit; Vector Laboratories, Burlingame, CA) and visualized using ECL substrate solution and ECL film (Amersham Biosciences, Piscataway, NJ).

2.5. Amino acid sequencing of the co-eluted protein

The piece cut from the gel was applied to endoproteinase Asp-N (Roche Diagnostics GmbH, Mannheim, Germany) digestion and the produced peptide fragments were separated by RP-HPLC using a MIC-15-03-MRP column (LC PACKING, San Francisco, CA) on SMART system (Amersham). Fragments were applied to Edman degradation by a LC system (492cLC, Applied Biosystems Japan, Tokyo, Japan) and a protein sequencer (PPSQ-10, Shimadzu, Kyoto, Japan). The co-eluted protein was identified by the N-terminal sequence determination of the fragments followed by the comparison with protein database SWISS-PROT.

2.6. Western blot analysis with anti-vimentin monoclonal antibodies

The complex containing Peptide-25N, and the co-eluted protein extracted above were applied to SDS–PAGE followed by silver staining or Western blot analysis with anti-vimentin monoclonal antibody (mAb), clone V9 (ICN Pharmaceuticals, Aurora, OH), HRP-linked whole anti-mouse IgG., ECL substrate solution, and ECL film (Amersham).

2.7. Binding assay of Peptide-25N to immobilized vimentin protein

The wells of 96-well black plates coated with 2 μg/mL of bovine vimentin (PROGEN, Heidelberg, Germany) were blocked with PBS containing 1% bovine serum albumin (PBS-BSA) for 2 h. Five microgram per milliliters of anti-vimentin mAb VIM3B (IgG2a) (PROGEN) or anti-α-actin mouse mAb clone ASM-1 (IgG2a) (PROGEN), or vehicle and then Peptide-25N solution was added. The wells were incubated with HRP-conjugated avidin (Amersham) in BSA-PBS for 1 h. After each step, wells were washed. The wells were incubated with ELISA Pico (Pierce) for 5 min. The chemiluminescence was detected using a plate reader (EnVision 2102 Multilabel reader, Perkin Elmer, Waltham, MA). In some experiments, the soluble vimentin was added in the presence of 1 μM Peptide-25N.

2.8. FACS analysis

To detect surface proteins, BAECs were harvested non-proteolytically by cell dissociation buffer (GIBCO BRL, Carlsbad, CA) and not permeabilized. The first Ab was 5 μg/mL of anti-bovine vimentin mAb clone VIM3B4 (IgG2a) or of mouse IgG2a and the second Ab was 8 μg/mL of fluorescein isothiocyanate (FITC)-conjugated anti-mouse IgG2a Ab (Santa Cruz Biotechnology, Santa Cruz, CA). Intact living cells which excluded propidium iodide were analyzed by FACS Vantage (Becton Dickinson, Bedford, MA). The difference in vimentin expression was evaluated by Kolmogrov–Smirnov test.

2.9. Binding assay of Peptide-25N to BAECs

Binding assays using BAECs were performed at 37 °C as described previously [9]. BAECs plated in a 96-well black plate were preincubated with 5 μg/mL of anti-bovine vimentin mouse mAb (clone VIM3B4) or with vehicle for 30 min. Cells were incubated for 60 min with 100 μg/mL of biotin-labeled or unlabeled peptide and then in HRP-conjugated streptavidin (Amersham) for further 30 min. the amount of bound peptide was detected by the addition of ECL Western blotting detection reagent (Amersham) and measured by Luminescencer JNR (Atto Co., Tokyo, Japan).

2.10. Wound migration assay

Wound migration assays were performed as described previously [9]. Cells were incubated with 100 μg/mL of peptide in preincubation (6 h) and in incubation (24 h) step after wounding. In some experiments, 5 μg/mL of anti-vimentin mouse mAb clone V9 (IgG1) (NeoMarkers, Fremont, CA) or of mouse IgG1 were added in both steps.

2.11. Statistical analysis

The statistical significance of differences in the data was evaluated by use of analysis of variance (ANOVA) and P values were calculated by Tukey's method. For comparison of two groups, the t-test was used. A value of $P < 0.05$ was accepted as statistically significant.

3. Results

To identify the membrane protein of binding partner for Peptide-25, the cross-linking experiment combined with avidin staining was performed (Fig. 1) and revealed a specific band bound to Peptide-25N in BAECs (the arrow in lane 1). This band was not detected in the absence of Peptide-25 in spite of the presence of Sulfo-EGS, a cross-linker (lane 2). Therefore, we decided to purify and identify this band as the target molecule bound to Peptide-25.

The membrane fraction was applied to avidin–biotin affinity chromatography and then SDS–PAGE (Fig. 1B). This target molecule (band A) and a co-eluted protein (band B) were further purified by SDS–PAGE. Firstly, the co-eluted protein with the consistent molecular size of 55 kDa [10] was identified as vimentin as a result of amino acid sequencing. To confirm it, the bands A and B were applied to Western blot analysis (Fig. 2). The band A (lanes 9 and 10) and the band B (lanes 6–8) reacted with an anti-vimentin mAb (Fig. 2). This result was reproduced, when another anti-vimentin mAb, clone VIM3B4, was used (data not shown). Therefore, we concluded that the target molecule to which Peptide-25N bound was vimentin (band B) and band A was the complex of vimentin and Peptide-25N (about 2.7 kDa).

We found that binding of Peptide-25 to EC surface was the key step for the augmented binding and activation of latent TGF-β [9]. To clarify whether vimentin is involved in this phenomenon, firstly we performed the binding assay. Peptide-25N bound to the immobilized vimentin protein in a dose dependent manner and anti-vimentin mAb (IgG2a) inhibited it, whereas anti-α-actin mAb, an irrelevant IgG2a, did not (Fig. 3A). Soluble vimentin suppressed the binding of Peptide-25N in a dose-dependent manner (Fig. 3B). These results indicate that vimentin could be a binding partner of Peptide-25. Next, we conducted FACS analysis using

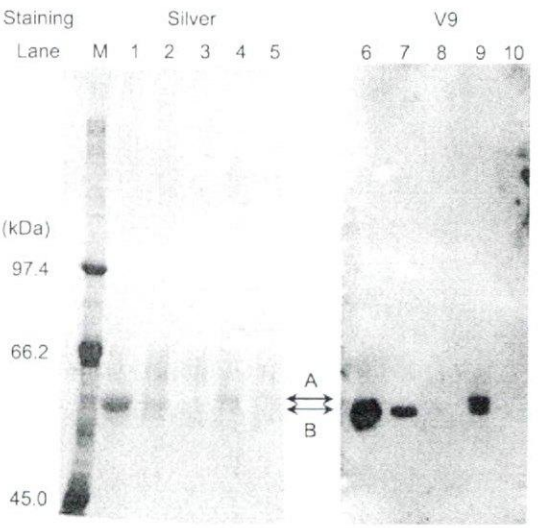

Fig. 2. Western blot analysis of the target fraction with anti-vimentin monoclonal antibody. Proteins from band A (lanes 4, 5, 9, and 10) and B (lanes 1–3 and 6–8) (Fig. 1B) were applied to SDS-PAGE followed by silver staining or Western blot analysis using anti-vimentin mAb, clone V9. The amount corresponding to culture area (cm^2): 119 for lanes 1, 4, 6, and 9; 11.9 for lanes 2, 5, 7, 10; 1.19 for lanes 3 and 8. The complex of Peptide-25N and its crosslinked protein, and the co-eluted protein were indicated by arrows A and B, respectively.

alive and membrane-intact BAECs and found that vimentin can exist on cell surface (Fig. 4A). Moreover, anti-vimentin mAb significantly suppressed the binding of peptide-25 to cells (Fig. 4B). These results indicate that Peptide-25 can directly and specifically interact with vimentin on cell surface.

Finally, we performed wound migration assay which is widely used to quantify activation of latent TGF-β [6,7,9,11,12]. Mature TGF-β, an active form, shows inhibitory activity to EC migration. Fig. 5 shows that Peptide-25 decreased the migration of ECs as we previously reported [9]. This inhibitory activity of Peptide-25 was attenuated by anti-vimentin mAb. In contrast to Peptide-25, Peptide-21 showed no significant activity (Fig. 5). Peptide-21 (from

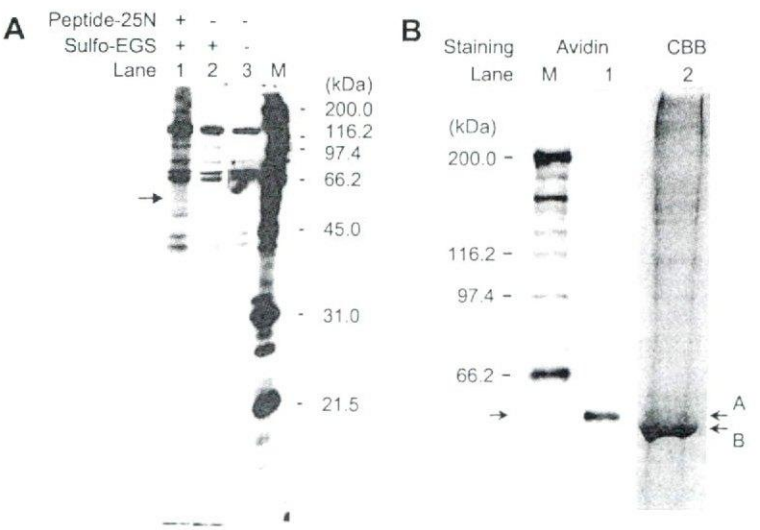

Fig. 1. Detection and purification of the target molecule of Peptide-25N. (A) Membrane fraction of BAEC was applied to SDS–PAGE with avidin staining and the candidate of the target molecule of Peptide-25N was detected (an arrow). (B) The target molecule fraction was obtained from the avidin–biotin affinity chromatography and applied onto SDS–PAGE followed by avidin (lane 1) or CBB staining (lane 2). Arrow A indicates the putative complex containing biotinylated Peptide-25N and arrow B does the co-eluted protein.